

Zirconium Phosphonate Frameworks Covalently Pillared with a Bipyridine Moiety

Fabrice Odobel,^{*,†} Bruno Bujoli,[†] and Dominique Massiot[‡]

Laboratoire de Synthèse Organique, Faculté des Sciences et des Techniques de Nantes, BP 92208, 44322 Nantes Cedex 03, France, and Centre de recherche sur les Matériaux des Hautes Températures, UPR CNRS 4212, 1D avenue de la Recherche Scientifique, 45071 Orléans Cedex 02, France

Received June 23, 2000. Revised Manuscript Received October 17, 2000

This paper describes for the first time the covalent immobilization of 5,5'-bis(dihydroxyphosphoryl)-2,2'-bipyridine ($\text{H}_2\text{O}_3\text{P-bipy-PO}_3\text{H}_2$: **1**) within the interlayer gallery of α and γ zirconium phosphonate structures. A mixed phosphite/phosphonate compound formulated as $\text{Zr}(\text{HPO}_3)_{0.8}(\text{O}_3\text{P-bipy-PO}_3)_{0.6}\cdot 5.3\text{H}_2\text{O}$ was obtained by reaction of 5,5'-bis(dihydroxyphosphoryl)-2,2'-bipyridine and phosphorous acid with $\text{ZrOCl}_2\cdot 8\text{H}_2\text{O}$ in the presence of HF. Another compound formulated as $\text{Zr}(\text{PO}_4)(\text{H}_2\text{PO}_4)_{0.5}(\text{HO}_3\text{P-bipy-PO}_3\text{H})_{0.25}\cdot 2\text{H}_2\text{O}$ was prepared by treatment of $\text{Zr}(\text{PO}_4)(\text{H}_2\text{PO}_4)\cdot 2\text{H}_2\text{O}$ (γ -ZrP) with 5,5'-bis(dihydroxyphosphoryl)-2,2'-bipyridine. These new materials have been characterized by X-ray powder diffraction, IR spectroscopy, thermogravimetry, one- and two-dimensional MAS ^{31}P NMR spectroscopy, and isothermal N_2 adsorption-desorption. The mixed α -zirconium phosphonate has a mesoporous area of $330\text{ m}^2/\text{g}$ (pore size, 40 \AA) and a microporous surface of $90\text{ m}^2/\text{g}$ whereas the pillared γ -ZrP phase is essentially microporous ($350\text{ m}^2/\text{g}$). Both materials display a narrow distribution of micropore size centered around 5 \AA . The metal binding of the bipyridine moieties remains intact after immobilization as shown by complexation experiments performed by contacting the solids with Cu(I) or Fe(II) methanolic solutions.

Introduction

One of the major challenges in materials sciences is the design and the development of hybrid organic–inorganic materials with tailor-made properties. These materials are based on the incorporation of functional active organic groups inside the inorganic framework and are often referred to as solids with a purpose. The hallmark features of these materials come from their ability to combine the properties of both the organic pendant groups along with those of the inorganic host.¹ Such an approach can result in the preparation of solids that can function as molecular sieves¹ of controlled pore size, shape-selective catalysts,² and molecular sorbents³ and can even provide a tailored reaction environment for included guest molecules.

Most industrial processes involve catalysis by transition metal complexes, which are generally dissolved in the reaction medium.⁴ However, if the catalyst is covalently anchored to an insoluble inorganic matrix, its recovery and its recycling become very easy to obtain with simple filtration. Besides this, if these materials are porous and the pore size can be controlled, the reagents can be selectively differentiated according to their shape and size. We thus embarked on a project aiming at designing materials that contain ligands capable of binding metal ions. To this purpose, we sought to incorporate the following features: (1) a strong organic ligand that can bind a wide variety of metal ions at different oxidation states, (2) a strong chemical link between the inorganic host and the organic ligand to ensure no leaching during the utilization of the solid, (3) a high chemical stability of the inorganic lattice to withstand multiple uses in a range of reaction conditions, and (4) an inorganic matrix with an open framework to permit diffusion and free access to most of the ligands immobilized inside the materials.

Among the inorganic matrixes currently employed for that endeavor, layered metal phosphonates⁵ have received growing interest during the past decade because their properties are suitable for fulfilling all the criteria listed above. More particularly, zirconium phosphonates are certainly the most suited materials for these ap-

* To whom correspondence should be addressed.

[†] Faculté des Sciences et des Techniques de Nantes.

[‡] Centre de recherche sur les Matériaux des Hautes Températures.

(1) Alberti, G. *Recent Development in Ion Exchange*; Williams, P. A., Hudson, M. J., Eds.; Elsevier Applied Science: London, 1987; pp 233–248.

(2) (a) Wan, B.-Z.; Anthony, R. G.; Peng, G. Z.; Clearfield, A. *J. Catal.* **1986**, *101*, 19–27. (b) Alberti, G.; Costantino, U. *J. Mol. Catal.* **1984**, *27*, 235–250. (c) Dines, M.; Digiacomo, P. M.; Callahan, K. P.; Griffith, P. C.; Lane, R. H.; Cooksey, R. E. *Proc. Am. Chem. Soc.* **1982**, *223*–240. (d) Callahan, K.; Dines, M. B. U.S. Patent, 4,983,564, 08/01/1991. (e) Deniaud, D.; Spyroulias, G. A.; Bartoli, J.; Battioni, P.; Mansuy, D.; Pinel, C.; Odobel, F.; Bujoli, B. *New J. Chem.* **1998**, *22*, 901–905.

(3) (a) Alberti, G. *Inorganic Ion Exchangers and Adsorbents for Chemical Processing in the Nuclear Fuel Cycle*; IAEA-TECDOC-337; IAEA: Vienna 1985; pp 195–211. (b) Cao, G.; Garcia, M. E.; Alcalá, M.; Burgess, L. F.; Mallouk, T. E. *J. Am. Chem. Soc.* **1992**, *114*, 7574–7575. (c) Mallouk, T. E.; Gavin, J. A. *Acc. Chem. Res.* **1998**, *31*, 209–217.

(4) (a) *Catalysis of Organic Reactions*; Rylander, P. N., Greenfield, H., Augustine, R. L., Eds.; Marcel Dekker Inc.: New York, 1988. (b) Noyori, R. In *Asymmetric Catalysis in Organic Synthesis*; John Wiley & Sons: New York, 1994.

plications because they are known to form very stable phosphonates, compatible in harsh conditions (basic, acidic, oxidative, or reductive) that can be employed during future uses of these solids.⁶ Furthermore, preparations and structural characterizations of zirconium phosphonates are well documented.

There are two different approaches for the inclusion of a phosphonic acid group inside a zirconium phosphonate framework. The first strategy consists of the coprecipitation of two different organic groups, one is a bisphosphonic acid that acts as a pillar to keep the two adjacent inorganic sheets further apart and the second is a small size phosphonic acid that creates an open space between the bridging units.^{5a,b,7} This usually leads to a structure of the α -type with the general formula, $Zr(O_3PRPO_3)_x(R'PO_3)_{2-2x} \cdot nH_2O$. The second approach is based on a direct topotactic reaction with an already formed γ -ZrP matrix, $Zr(H_2PO_4)(PO_4) \cdot 2H_2O$. During this reaction, part of the original $H_2PO_4^-$ groups of γ -ZrP are replaced by the phosphonic acid with no significant modification of the structure.⁸

Both strategies have been successfully used by Clearfield and co-worker⁹ and Brunet and co-worker¹⁰ for the covalent immobilization of crown ethers phosphonates. With these immobilized macrocyclic polyethers, selective binding of alkaline cations could be achieved. The bidentate heteroaromatic ligand 2,2'-bipyridine is among the best known coordinating agents.¹¹ This highly studied multidentate nitrogen ligand affords tight binding for metal cations due to the chelate effect and the π -accepting ability of this moiety. Hence, its covalent immobilization within insoluble porous materials is an appealing endeavor.

Herein, we describe the preparation and the characterization of novel zirconium phosphonates incorporating covalently attached 5,5'-bis(dihydroxyphosphoryl)-2,2'-bipyridine as a potential binding site for a variety of transition metals.¹²

Recently, Tomlinson and others reported the entrapment of polypyridine molecules in an α -ZrP framework via acid-base interactions.¹³ A real advantage of the approach developed in the present work is that the strong covalent bonds with the inorganic matrix prohibited leaching of the bipyridine group during the utilization of the materials. Furthermore, a diverse variety of pillar lengths can be exploited to adjust the interlayer distance systematically to control the pore diameter.

The present paper gives a full account of the immobilization of 5,5'-bis(dihydroxyphosphoryl)-2,2'-bipyridine (1) within an α - and γ -type ZrP with a detailed characterization of the resulting phases as well as their complexing properties.

Preparation of the Materials

α -Zirconium Phosphite(2,2'-bipyridine-5,5'-diphosphonate). The preparation of this type of zirconium phosphonate structure is closely related to the standard method already developed by Clearfield^{5b} and Alberti^{7a,c} groups. It involves the utilization of HF as complexing agent of zirconium. The slow displacement of the fluoride concentration during the reaction, which leads to the precipitation of the zirconium phosphonate, is made by controlling its evaporation by a gentle heating. Dimethyl sulfoxide has been used as solvent because it solubilizes all the reagents, especially organo-phosphonic acids which are generally insoluble in most common solvents.

Zirconium has been chosen for this study because of the already mentioned properties but also because its oxophilic properties will not cause any complexation competition with the nitrogen bipyridine coordination site. Indeed, if divalent metal ions such as zinc or copper were used, it is highly likely that during the preparation of the solid coordination of the metal ion would take place with both the phosphonic acid and bipyridine moieties, leading to a solid with no complexing capacity.

The preparation of porous materials requires a second phosphorus-based acid of small size to be copolymerized with the bipyridine bis-phosphonic acid. Phosphorous acid has been preferred to phosphoric acid because of its smaller bulkiness and because the phosphite proton cannot be exchanged with metal ions.^{6,7b} Thus, uptake of metal ions can arise only from a bipyridine chelating center and not from ion exchange reactions with the acidic proton of the inorganic phase.

Several experiments with different phosphorous acid to bipyridine molar ratios have been carried out. The results of the preparations are gathered in Table 1.

The following points are noteworthy:

(1) If the molar ratio " r " is equal or above 25, there is formation of α -Zr(HPO₃)₂·2H₂O in addition to the mixed pillared phase. This is evidenced by an X-ray powder diffraction pattern in which characteristic peaks of this latter phase are apparent ($d = 5.6 \text{ \AA}$).

(5) (a) Alberti, G. *Comprehensive Supramolecular Chemistry*, 7; Pergamon Press: New York, 1996; pp 151–185. (b) Clearfield, A. In *Progress in Inorganic Chemistry*; Karlin, K. D., Ed.; John Wiley & Sons: New York, 1998; Vol. 47, pp 371–510. (c) Cao, G.; Hong, H.-G.; Mallouk T. E. *Acc. Chem. Res.* **1992**, *25*, 420–427. (d) Alberti, G.; Costantino, U.; Dionigi, C.; Murcia-Mascaros, S.; Vivani, R. *Supramol. Chem.* **1994**, *6*, 29–40. (e) Alberti, G.; Costantino, U.; Vivani, R. *Adv. Mater.* **1996**, *8*, 291–303.

(6) Olivera-Pastor, P.; Maireles-Torres, P.; Rodriguez-Castellon, E.; Jimenez-Lopez A. *Chem. Mater.* **1996**, *8*, 1758–1769.

(7) (a) Alberti, G.; Costantino, U.; Környei, J.; Luciani, M. L.; Giovanotti, L. *React. Polym.* **1985**, *4*, 1–10. (b) Costantino, U.; Nocchetti, M.; Marmottini, F.; Vivani, R. *Eur. J. Inorg. Chem.* **1998**, 1447–1452. (c) Rosenthal, G. L.; Caruso, J. J. *Solid State Chem.* **1993**, *107*, 497–502. (d) Medoukali, D.; Mutin, P. H.; Vioux A. *J. Mater. Chem.* **1999**, *9*, 2553–2557. (e) Alberti, G.; Costantino, U.; Giulietti, R. *Gazz. Chim. Ital.* **1983**, *113*, 547–552.

(8) (a) Alberti, G.; Giontella E.; Murcia-Mascaros, S.; Vivani R. *Inorg. Chem.* **1998**, *37*, 4672–4676. (b) Alberti, G.; Giontella E.; Murcia-Mascaros, S. *Inorg. Chem.* **1997**, *36*, 2844–2849. (c) Yamanaka, S.; Sakamoto, K.; Hattori, M. *J. Phys. Chem.* **1984**, *88*, 2067–2070. (d) Alberti, G.; Vivani R.; Biswas, R. K.; Murcia-Mascaros, S. *React. Polym.* **1993**, *19*, 1–12. (e) Alberti, G.; Murcia-Mascaros, S.; Vivani, R. *Mater. Chem. Phys.* **1993**, *35*, 187–192. (f) Yamanaka, S.; Hattori, M. *Inorg. Chem.* **1981**, *20*, 1929–1931. (f) Alberti, G.; Murcia-Mascaros, S.; Vivani R. *J. Am. Chem. Soc.* **1998**, *120*, 9291–9295.

(9) Zhang, B.; Clearfield, A. *J. Am. Chem. Soc.* **1997**, *119*, 2751–2752.

(10) (a) Brunet, E.; Huelva, M.; Rodriguez-Ubis, J. C. *Tetrahedron Lett.* **1994**, *35*, 8697–8700. (b) Brunet, E.; Huelva, M.; Vázquez R.; Juanes, O.; Rodriguez-Ubis, J. C. *Chem. Eur. J.* **1996**, *2*, 1578–1584.

(11) Cotton, F. A.; Wilkinson, G. *Advanced Inorganic Chemistry*; John Wiley and Sons: Singapore, 1988.

(12) Penicaud, V.; Odobel, F.; Bujoli B. *Tetrahedron Lett.* **1998**, *39*, 3689–3692.

(13) (a) Ferragina, C.; Ginestra, A. L.; Massucci, M. A.; Patrono, P.; Tomlinson, A. G. *J. Phys. Chem.* **1985**, *89*, 4762–4769. (b) Ferragina, A. L.; Massucci, M. A.; Patrono, P.; Al Ginestra, A.; Tomlinson, A. A. *J. Chem. Soc., Dalton Trans* **1986**, 265–271. (c) Ferragina, A. L.; Massucci, M. A.; Patrono, P.; Al Ginestra, A.; Tomlinson, A. A. *J. Chem. Soc., Dalton Trans.* **1988**, 851–857.

(14) Zhang, B.; Poojary, D. M.; Clearfield, A. *Inorg. Chem.* **1998**, *37*, 1844–1852.

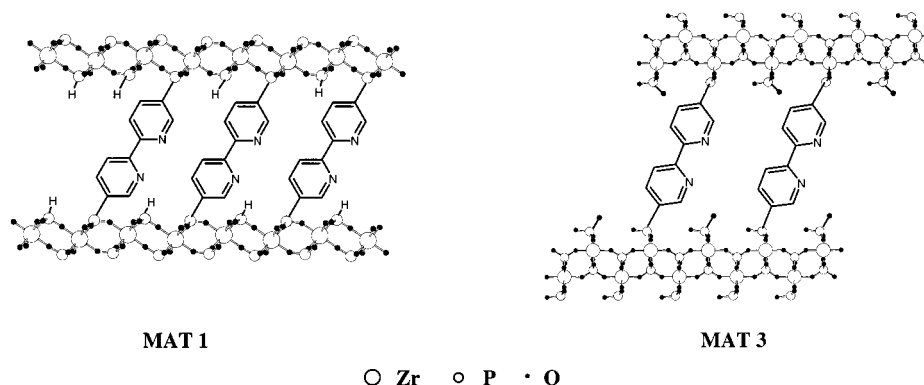


Figure 1. Idealized schematic representation of the structure of the pillared layered compounds prepared from bipyridine **1**: by self-assembling with $\text{ZrOCl}_2 \cdot 8\text{H}_2\text{O}$ and H_3PO_3 (right); by intercalation of **1** in $\gamma\text{-ZrP}$ (left).

Table 1. Results of the Experiments Made for the Preparation of the Mixed Zirconium Phosphite/Phosphonate; Reactions Were Performed in DMSO Using $\text{HF/Zr} = 17$ and $\text{P/Zr} = 4$

designation	$r^a = \text{H}_3\text{PO}_3/\text{bipyridine (1)}$	composition of the solid
MAT 1	5	single phase of composition: $\text{Zr}(\text{HPO}_3)_{0.8}(\text{O}_3\text{P-bipy-PO}_3)_{0.6} \cdot 5.3\text{H}_2\text{O}$
	10	
	15	
	25	mixture of several phases including $\text{Zr}(\text{HPO}_3)_2 \cdot 2\text{H}_2\text{O}$
	35	
	50	

^a r is the initial molar ratio.

(2) Within the interval molar ratio $5 \leq r \leq 15$, a single solid phase was formed and its composition remains almost constant, whatever the initial ratio r . The resulting solid has the following formulation: $\text{Zr}(\text{HPO}_3)_{0.8}(\text{O}_3\text{P-bipy-PO}_3)_{0.6} \cdot 5.3\text{H}_2\text{O}$ (MAT 1).

These results indicate, as already reported by Clearfield and co-workers¹⁴ and Alberti and co-workers¹⁵ for the preparation of mixed phosphonates, that it is not always possible to cover a linear range of concentration of pillars in the solid phase and it is especially difficult to dilute it significantly. The material obtained here contains one pillar for roughly one phosphorous acid unit. An attempt to increase this ratio by increasing the concentration of H_3PO_3 leads to the formation of $\text{Zr}(\text{HPO}_3)_2 \cdot 2\text{H}_2\text{O}$ along with the mixed component phosphonate.

γ -Zirconium Phosphate Pillared with Bipyridine Units. Another appealing way to immobilize our bipyridine bisphosphonic precursor is its covalent intercalation inside $\gamma\text{-ZrP}$ via topotactic exchange.⁸ The reaction proceeds efficiently following the usual refluxing conditions reported by Alberti in an acetone/water (1/1) mixture.^{8a,b,16}

Two molar ratios between bipyridine diphosphonic acid and $\gamma\text{-ZrP}$ have been investigated. The composition of the two resulting solids are gathered in Table 2. A higher percentage of intercalation has not been explored since Alberti and co-workers have already demonstrated that the maximum microporous surface that can be

Table 2. Results of the Experiments Made for the Preparation of the Mixed Zirconium Phosphate/Phosphonates from $\gamma\text{-ZrP}$; Reactions Were Carried Out in Water/Acetone: 1/1

designation	$r^a = \gamma\text{-ZrP}/\text{bipyridine (1)}$	composition of the solid
MAT 2	1.65	$\text{Zr}(\text{PO}_4)(\text{H}_2\text{PO}_4)_{0.8}(\text{HO}_3\text{P-bipy-PO}_3\text{H})_{0.1} \cdot 2\text{H}_2\text{O}$
MAT 3	3.3	$\text{Zr}(\text{PO}_4)(\text{H}_2\text{PO}_4)_{0.5}(\text{HO}_3\text{P-bipy-PO}_3\text{H})_{0.25} \cdot 2\text{H}_2\text{O}$

^a r is the initial molar ratio.

achieved using biphenyl bisphosphonic acid corresponds to roughly 30% of pillaring.¹⁶

The percentage of H_2PO_4^- replaced by bipyridine diphosphonic acid **1** is proportional to the initial amount of reacted bipyridine. Contrary to the previous method, this second approach makes it possible to control the percentage of bipyridine pillars inside the interlayer space. This feature is essential because it is generally accepted that the control of the microporous volume depends on the possibility of modulating the concentration of the pillaring groups because the micropore size is directly proportional to the mean distance between two neighboring pillars.

Powder X-ray Diffraction Study

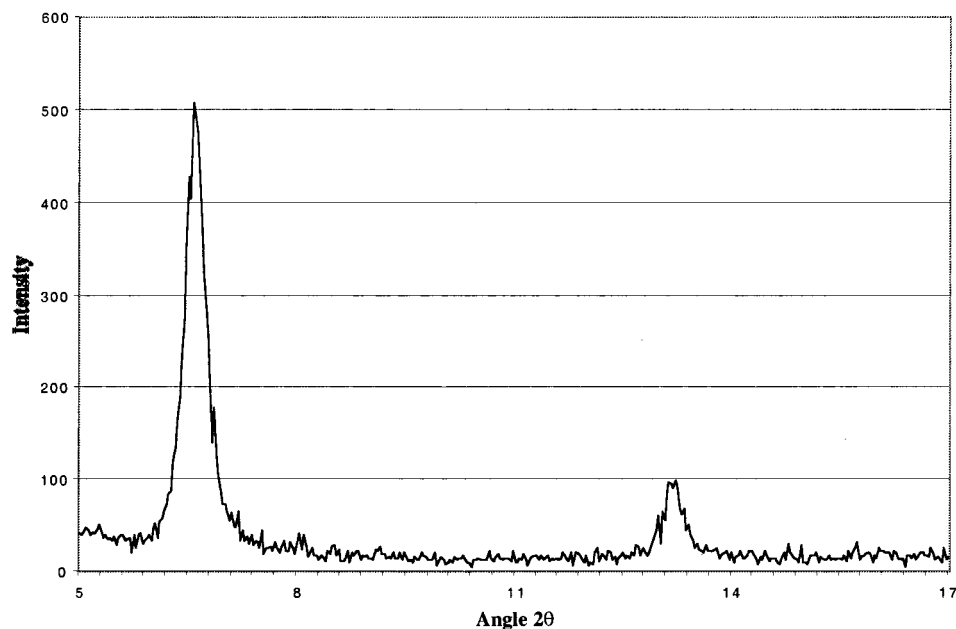
To gain information on the crystallinity and the structure of the materials, XRD patterns of every sample were systematically recorded. No single crystal for X-ray structural determination was obtained but speculation on the structure of these compounds can be confidently made from existing knowledge of the structure of aryl bisphosphonates homologues. As already described in the literature, the general trend is the formation of a two-dimensional pillared structure in which the organic bisphosphonic acid groups link adjacent inorganic sheets. An idealized representation of the structure of these materials is given in Figure 1.

The diffraction diagrams of the materials are depicted in Figure 2. The crystallinity estimated from the X-ray powder patterns is good because the diffraction peaks are relatively narrow. However, for MAT 1, it is appreciably lower than that for MAT 2–3.

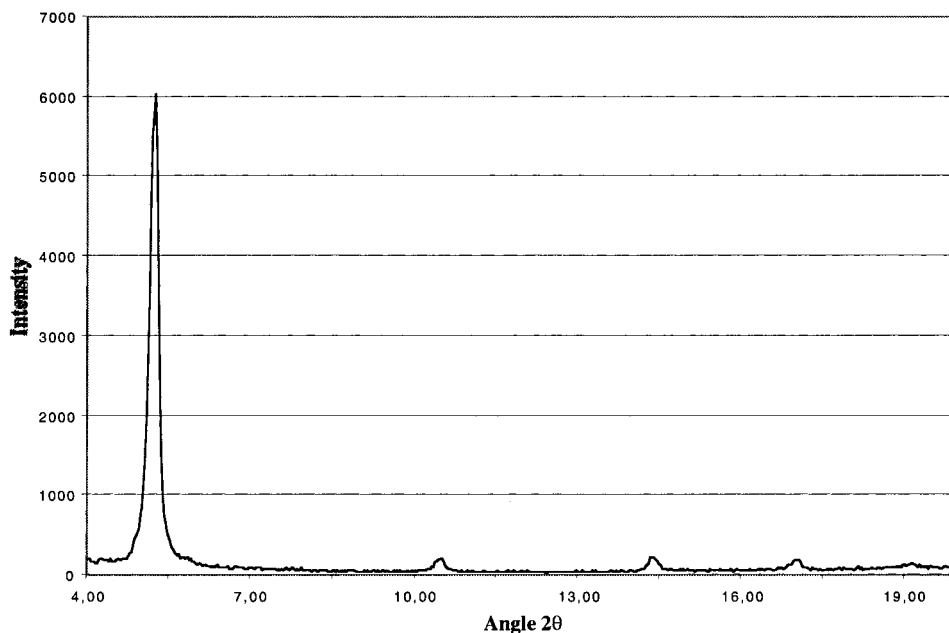
The d spacing of the resulting phases is given in Table 3. They are in good agreement with similar materials pillared with biphenyl diphosphonate, which are reported to be 13.9 and 16.5 Å for a mixed zirconium phosphonate of α -type and $\gamma\text{-ZrP}$, respectively. The interlayer distance (13.4 Å) in the mixed material (MAT 1) is identical to the one of the pure α -zirconium

(15) (a) Alberti, G.; Costantino, U.; Vivani, R.; Zappelli, P. Eur. Patent, EP 0492694B1; 16/10/1996, Appl01/07/1992, 38 pp. (b) Alberti, G.; Costantino, U.; Vivani, R.; Zappelli, P.; Rossodivita, A.; Bassignagni, L. Eur. Patent, 0469682B1; 14/12/94, Appl05/02/1992, 22 pp.

(16) (a) Alberti, G.; Marmottini, F.; Murcia-Mascaros, S.; Vivani, R. *Angew. Chem., Int. Ed. Engl.* **1994**, *33*, 1594–1597. (b) Penicaud, V.; Massiot, D.; Gelbart, G.; Odobel, F.; Bujoli, B. *J. Mol. Struct.* **1998**, *470*, 31–38.



MAT 1



MAT 3

Figure 2. X-ray diffraction patterns of the zirconium phosphonates MAT 1 and MAT 3.

Table 3. Interlayer Spacings of the Mixed Materials MAT 1–3 and the Corresponding Single-Component Products

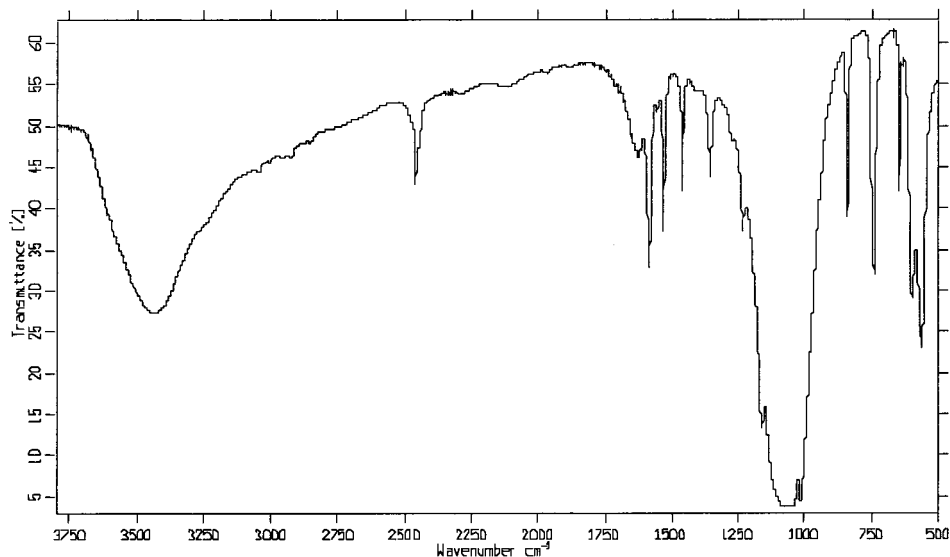
designation	composition of the solid	<i>d</i> spacing
MAT 4	Zr(HPO ₃) ₂ ·2H ₂ O	<i>d</i> = 5.6 Å
MAT 5	Zr(O ₃ P-bipy-PO ₃)·3H ₂ O	<i>d</i> = 13.4 Å
MAT 1	Zr(HPO ₃) _{0.8} (O ₃ P-bipy-PO ₃) _{0.6} ·5.3H ₂ O	<i>d</i> = 13.4 Å
γ-ZrP	Zr(PO ₄)(H ₂ PO ₄)·2H ₂ O	<i>d</i> = 12.2 Å
MAT 2	Zr(PO ₄)(H ₂ PO ₄) _{0.8} (HO ₃ P-bipy-PO ₃ H) _{0.1} ·2H ₂ O	<i>d</i> = 16.2 Å
MAT 3	Zr(PO ₄)(H ₂ PO ₄) _{0.5} (HO ₃ P-bipy-PO ₃ H) _{0.25} ·2H ₂ O	<i>d</i> = 16.9 Å

bipyridine bisphosphonate material (MAT 5). This is a fine confirmation that the bipyridine is really present in the interlayer space acting as a pillar.

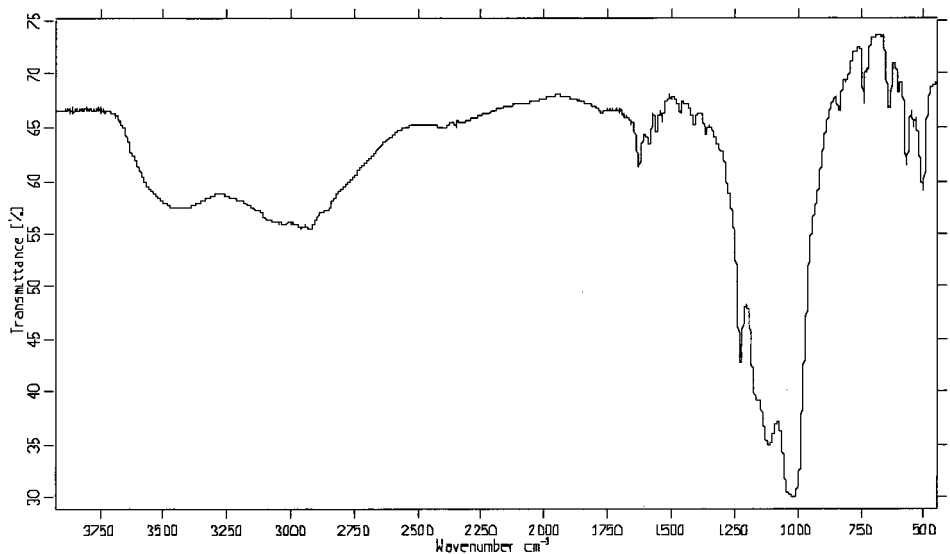
The length of the bipyridine pillar, estimated from CPK models, is 13.6 Å measured from the oxygen of the two opposite PO₃H₂ groups. Knowing that the thickness of the inorganic sheet is respectively ≈6.3 and ≈9.1 Å for the α-ZrP⁹ and γ-ZrP^{8f} structural types, the free

space available in the gallery is, therefore, ≈7.1 and 7.8 Å for MAT 1 and MAT 3, respectively. It can be concluded that the bipyridine is not oriented perpendicular to the layer, but it is inclined at an angle of ≈35° and 32° relative to the mean plane of the zirconium layer in MAT 1 and MAT 3, respectively.

It is instructive to compare the basal spacing of these covalently pillared materials with those made by simple intercalation of 2,2'-bipyridine in a zirconium phosphate via acid–base interactions.¹³ In the latter case, the interlayer found was 10.9 Å, consistent with a flat orientation of the bipyridine moiety interacting through H-bonding with the acidic phosphate protons of the matrix. The basal spacing of 13.4 Å, found in the covalently pillared α-ZrP material MAT 1, is additional confirmation of the lengthwise orientation of the bipy-



MAT 1



MAT 3

Figure 3. IR spectra of samples MAT 1 and MAT 3 recorded in KBr pellets.

ridine, which allows free access to the bipyridine chelating nitrogens.

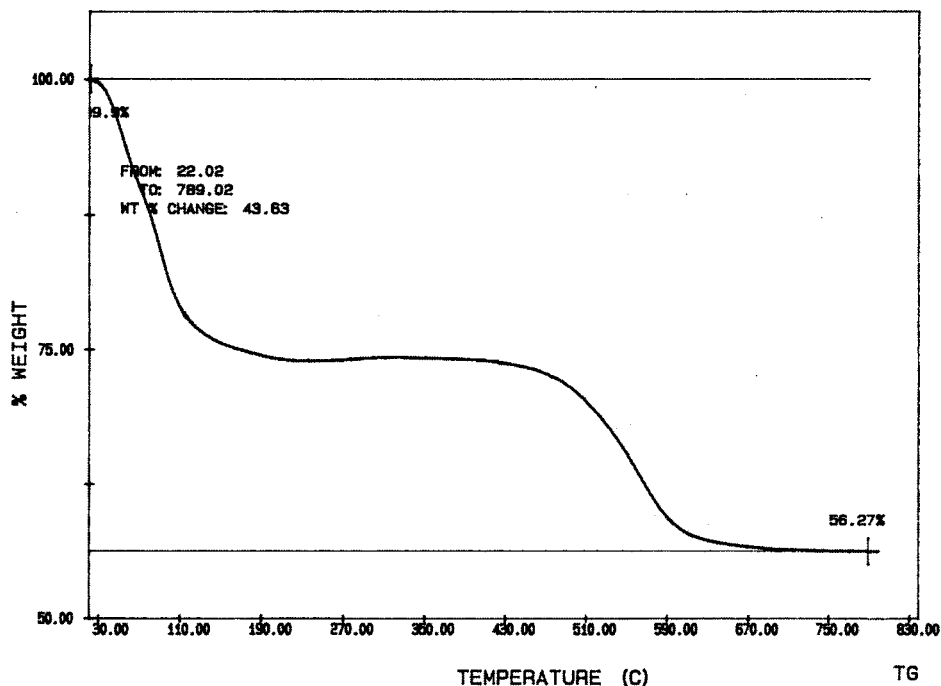
Infrared Spectroscopy

Infrared spectra were recorded to gain further insight into the protonation state of the bipyridine and the nature of the solvents present inside the pores (Figure 3). The broad band at 3440 cm^{-1} and the sharp band at 1630 cm^{-1} are indicative of water adsorbed inside the materials. It is interesting to detect this band with a high absorption level, even in MAT 1, which would be expected to be highly hydrophobic because of the large organic matter content. There is no significant amount of residual dimethyl sulfoxide in the materials because its signature, given by the characteristic doublet at 1410 and 1438 cm^{-1} , is not observed in any spectrum.

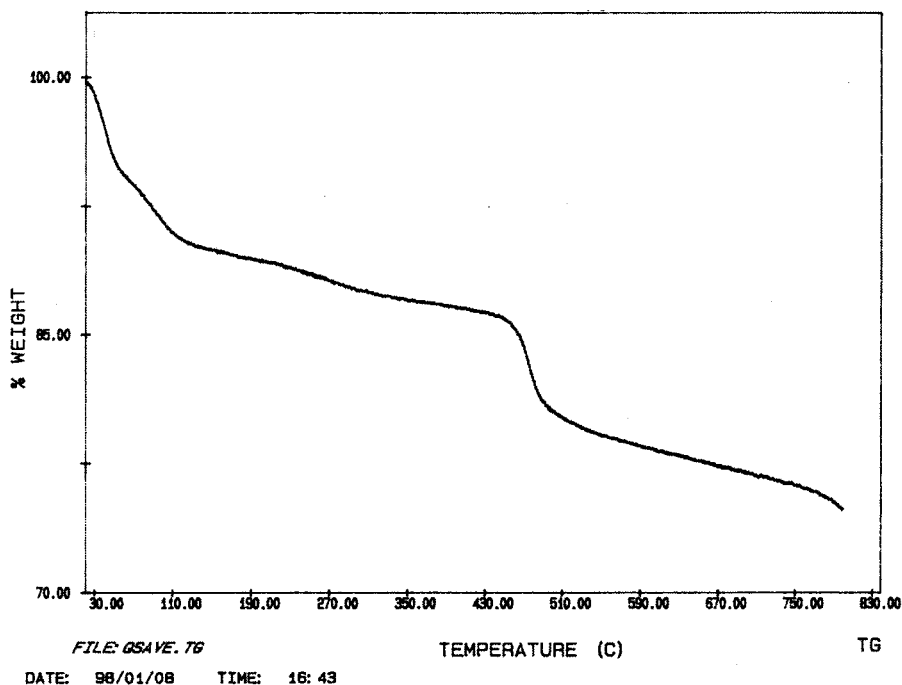
The other informative region in the spectrum is located between 1400 and 1600 cm^{-1} and corresponds to the stretching vibration modes of the bipyridine ring. To properly assign the bands of this region, the spectra

of the protonated and neutral form of bipyridine have been recorded. The bands at 1577 and 1276 cm^{-1} are characteristic of the pyridinium ion whereas those at 1461 , 1390 , and 1276 cm^{-1} are indicative of the free bipyridine. In the IR spectra of all materials, the only resonances could be detected are those of the free bipyridine, suggesting that the intercalated bipyridine is mostly unprotonated, although traces of protonated species may also exist.

The signature of the phosphite group can be clearly seen at 2456 cm^{-1} in the spectrum of MAT 1. This medium intensity band corresponds to the stretching vibration of the P–H bond and it has been shifted compared to the pure zirconium phosphite phase (doublet at 2347 and 2388 cm^{-1}). This shift is due to a different chemical environment of the phosphite group in the mixed phosphite/phosphonate compared to $\text{Zr}(\text{HPO}_3)_2 \cdot 2\text{H}_2\text{O}$. This supports the hypothesis that HPO_3 and $\text{bipy}(\text{PO}_3)_2$ blocks are effectively mixed together and that no phase separation has occurred. In MAT 3, the broad band located between 2900 and 3100 cm^{-1} is



MAT 1



MAT 3

Figure 4. Thermogravimetric analysis curves for compounds MAT 1 and MAT 3.

due to the stretching mode of the hydroxy group present on the phosphate and phosphonate moieties of the modified γ -ZrP.

The lower wavelength region between 1200 and 800 cm^{-1} is composed of strong bands that can be attributed to $\nu(\text{P}-\text{O})$ vibrations. Particularly interesting is the strong and broad band at 1060 cm^{-1} , which is characteristic of the α -type zirconium phosphonate compounds and is assigned to the vibration of the PO_3^{2-} group.¹⁷

(17) Wang, J. D.; Clearfield, A.; Peng, G.-Z. *Mater. Chem. Phys.* **1993**, *35*, 208–216.

Thermogravimetric Study

TGA traces of materials MAT 1 and MAT 3 have been obtained under air sweeping and are shown in Figure 4. For both materials, the first weight loss occurs around 40 °C and is due to water desorption. It corresponds to 5.3 and 2 molecules of water of hydration for MAT 1 and MAT 3, respectively. The second weight loss occurs around 500 °C and is due to the thermal decomposition of the organic moieties, leading to the formation of inorganic zirconium (most probably ZrP_2O_7 or ZrO_2) along with CO_2 and H_2O . It is important to note that the thermal stability of the bipyridine has increased

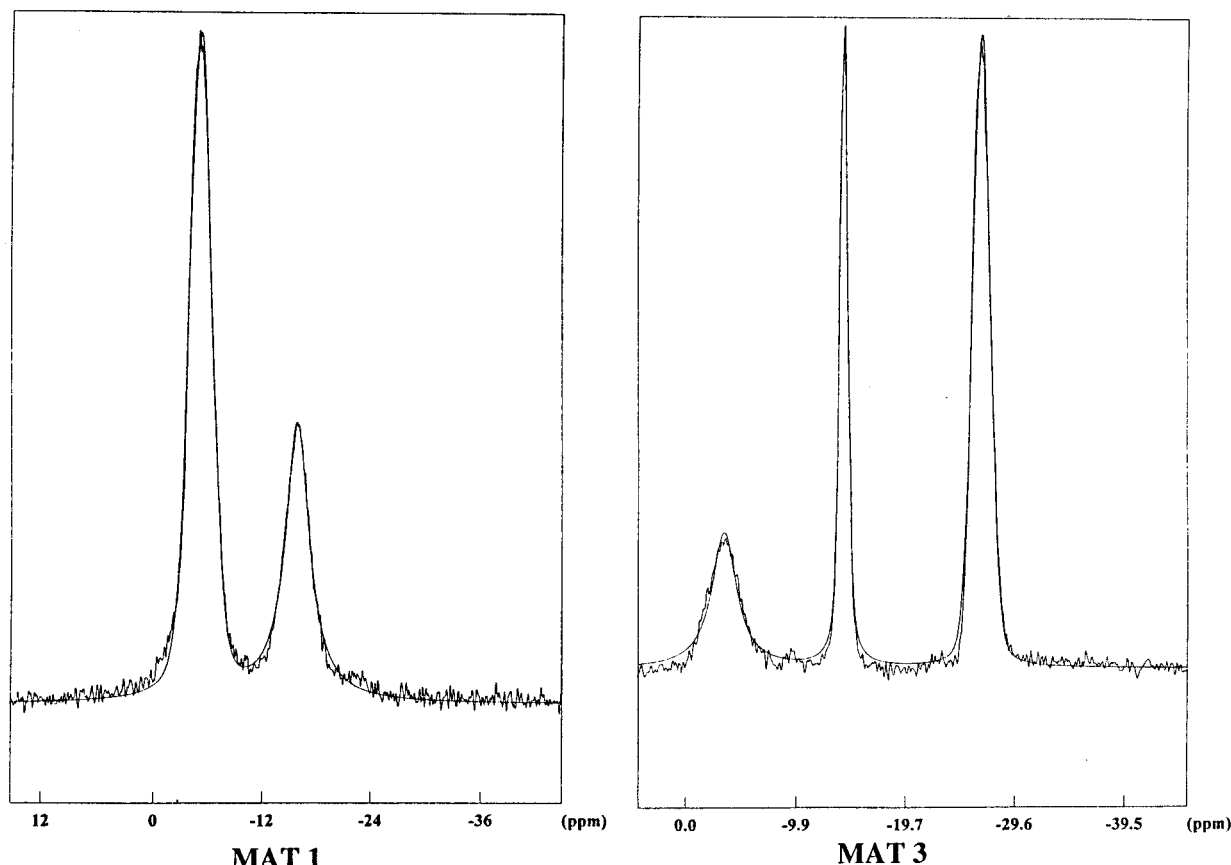


Figure 5. Solid-state ^{31}P MAS NMR spectra of materials MAT 1 and MAT 3.

Table 4. Characteristics of the Solid-State ^{31}P MAS NMR Spectra of Materials MAT 1–5

designation	δ_1 (ppm)	$\Delta\delta_1^a$ (Hz)	$S(\delta_1)$	δ_2	$\Delta\delta_2^a$ (Hz)	$S(\delta_2)$	δ_3	$\Delta\delta_3^a$ (Hz)	$S(\delta_3)$
MAT 4				-15.8	335	100%			
MAT 5	-4.2	334	100%						
MAT 1	-5.1	358	63%	-15.9	393	37%			
γ -ZrP				-9.5	75	50%	-27.4	53	50%
MAT 2	-3.5	347	9%	-14.3	93	37%	-26.9	219	54%
MAT 3	-3.6	325	24%	-14.2	102	24%	-26.7	224	52%

^a Full width at half-maximum.

significantly once immobilized inside the inorganic framework. This is one of the possible advantages of immobilizing organic species and it will be really beneficial for potential technological applications such as catalysis.

NMR Spectroscopy

The ^{31}P MAS NMR spectra of the materials MAT 1 and MAT 3 are shown in Figure 5. The attributions of the spectra were made according to the chemical shifts found in the pure zirconium phosphite (MAT 4), zirconium phosphonate (MAT 5), and γ -ZrP (Table 4).

In MAT 1 two major resonances are observed, one corresponding to the phosphonic acid group of bipyridine (-5.1 ppm) and the other to the phosphite group (-15.9 ppm). As expected, three ^{31}P resonances are present for MAT 2 and MAT 3, -3.5 ppm (intercalated bipyridine diphosphonic acid), -14.2 ppm (residual exchangeable H_2PO_4), and -26.7 ppm for the nonexchangeable PO_4^{3-} , in full agreement with the values found for other

pillared γ phases previously described.¹⁸

One important conclusion that can be drawn from ^{31}P NMR spectra is that all phosphonic groups are bonded to zirconium because there is only one resonance per organo-phosphonate group for every sample. Generally, when the solid contains either bonded and free phosphonic groups, several signals appear in the spectrum with the free phosphonic group being deshielded relative to the coordinated one. This is also sustained by the measurement of the P/Zr ratio by EDX, which was constantly found to be equal to 2.

The formulations of compounds MAT 1–MAT 3 deduced from the solid-state NMR measurements agreed well with the composition determined by liquid NMR after solubilization of the samples in a $\text{HF}/\text{D}_2\text{O}$ mixture.

Moreover, the full width at half-maximum (fwhm) of the signals are comparable to those observed for the three references (MAT 4–5 and γ -ZrP) for which a good crystallinity was evidenced by XRD. Consequently, this suggests that the mixed component phases are homogeneous and relatively well ordered. In addition, a two-dimensional ^{31}P exchange experiment was performed to give deeper insight to the local structure of MAT 1. Two types of experiments were carried out, with and without proton decoupling during the mixing period.¹⁹ When proton decoupling is applied, the two sites of MAT 1 show up along the diagonal line. For a 1-s mixing time, an exchange figure (off-diagonal cross peaks in the two-dimensional contour plots in which the two sites are

(18) Clayden, N. J. *J. Chem. Soc., Dalton Trans.* **1987**, 1877–1880.
 (19) Schmidt-Rohr, K. W.; Spiess, H. *Multidimensional Solid-State NMR and Polymers*; Academic Press: New York, 1994.

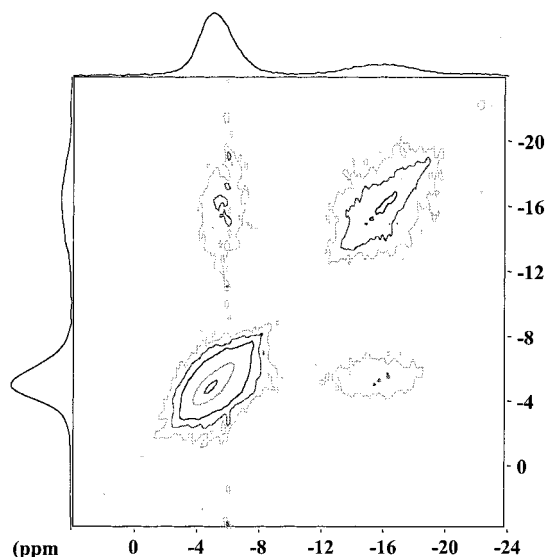


Figure 6. ^{31}P ^{31}P proton-mediated two-dimensional MAS NMR exchange spectrum of MAT 1.

Table 5. Surface Area Measurements for MAT 1–5^a

	total BET surface area	mesoporous surface	mean mesopore diameter	microporous surface	mean micropore diameter
MAT 4	10 m ² /g	n.d.	n.d.	n.d.	n.d.
MAT 5	130 m ² /g	130 m ² /g	40 Å	0	0
MAT 1	420 m ² /g	330 m ² /g	40 Å	90 m ² /g	5 Å
γ -ZrP	10 m ² /g	n.d.	n.d.	n.d.	n.d.
MAT 3	380 m ² /g	0	0	350 m ² /g	5 Å
MAT 2	60 m ² /g	n.d.	n.d.	n.d.	n.d.

^a n.d. = not determined.

involved) is present when proton decoupling is turned off during the mixing time. The exchange process is driven by ^1H spin diffusion and this unambiguously shows that the two observed phosphorus species are intimately mixed at the molecular scale, thus confirming that MAT 1 is a single phase (Figure 6).

Surface Area and Porosity measurements

The results of the surface area and the pore volume determination were investigated using nitrogen adsorption–desorption isotherms (Table 5). Clearly, the pillared materials have high surface areas with values ranging from 380 to 420 m²/g, significantly higher than those of the three references MAT 4, MAT 5, and the unexchanged γ -ZrP phase. However, the pure bipyridine zirconium phosphonate phase (MAT 5) exhibits a noticeable surface area, which essentially arises from mesoporosity.

Mesopores are most probably due to aggregation of small solid particles, which creates little cavities. The traces of the adsorption isotherms of MAT 1 and MAT 3 are shown in Figure 7. For MAT 1, it exhibits the expected hysteresis loop, indicative of porosity in the mesopore domain. The Horvath–Kawazoe differential pore volume plot and the micropore distribution are illustrated in Figure 8.

The microporosity detected in MAT 1 and MAT 3 is attributed to the open space between the bipyridine pillars inside the interlayer gallery. The average diameter of 5 Å is very close to the value found by Alberti and co-workers in zirconium phosphite(3,3',5,5'-tetram-

ethylbiphenyl)diphosphonate²⁰ or in the γ -ZrP phase intercalated with a biphenyl diphosphonate pillar.¹⁶ Therefore, it can be concluded that the microporosity in our samples has the same origin as the one found in Alberti's materials.

The porosity of the materials obtained with the copolymerization technique is essentially in the mesopore region with an average diameter of 40 Å. This result can be attributed to a content of pillars that is too high to leave free room in the interlayer region. However, an appreciable amount of microporous surface with a narrow distribution size centered around 5 Å has been produced, especially in the case of MAT 3. Although further investigations are necessary to prepare larger pore size materials for catalysis, these preliminary results are encouraging and show that microporous materials with high surface area can be prepared with pillared metal phosphonates.

Metal Ion Uptake by the Bipyridine-Containing Phosphonates

One of the most interesting features of these bipyridine-based phosphonates materials is their potential binding properties for removal of metals from industrial wastes toward a trace-metal-free environment or for the preparation of supported homogeneous catalysts.

The complexing ability of the bipyridine units after immobilization was examined by exposing the solids to a methanol solution of iron(II) or copper(I). Bipyridine is an excellent ligand for most transition metals, but iron(II) and copper(I) have been chosen for this study because the corresponding complexes are known to be very colored.²¹ Therefore, an easy qualitative characterization of the metal binding can be done on the grounds of their electronic absorption spectra. Contact of MAT 1 and MAT 3 with the metal salt solutions instantly resulted in a color change from white to pink with iron(II) and from white to brown with copper(I). The Fe(II) and Cu(I) cations are known to form spontaneously octahedral and tetrahedral complexes with three and two bipyridine units, respectively. In MAT 1 and MAT 3, it seems reasonable to assume that such a stoichiometry cannot be achieved because bipyridine is covalently pillared on both ends; therefore, the cations cannot be bound by more than one bipyridine pillar. Furthermore, after ion binding, EDX measurements on the solids demonstrated that the Cu/Zr and Fe/Zr ratios correspond to the loading level of bipyridine, indicating that there is only one metal bound per bipyridine unit.

The UV–vis absorption spectra of the resulting materials and those of the iron(II) and copper(I) bipyridine complexes in solution are shown in Figure 9. These spectra are characterized by a broad and intense band characteristic of the metal-to-ligand charge-transfer (MLCT) transition. This transition is known to also arise in complexes containing one, two, or three bipyridines, but the exact position of this band changes substantially according to the ligand sphere around the metal (number of ligands that can be either solvent,

(20) Alberti, G.; Costantino, U.; Marmottini, F.; Vivani R.; Zappelli, P. *Angew. Chem., Int. Ed. Engl.* **1993**, *32*, 1357–1359.

(21) (a) Janiak, C.; Deblon, S.; Wu, H.-P.; Kolm, M. J.; Klüfers, P.; Piotrowski, H.; Mayer, P. *Eur. J. Inorg. Chem.* **1999**, 1507–1521. (b) Zhu, S. S.; Swager, T. M. *J. Am. Chem. Soc.* **1997**, *119*, 12568–12577.

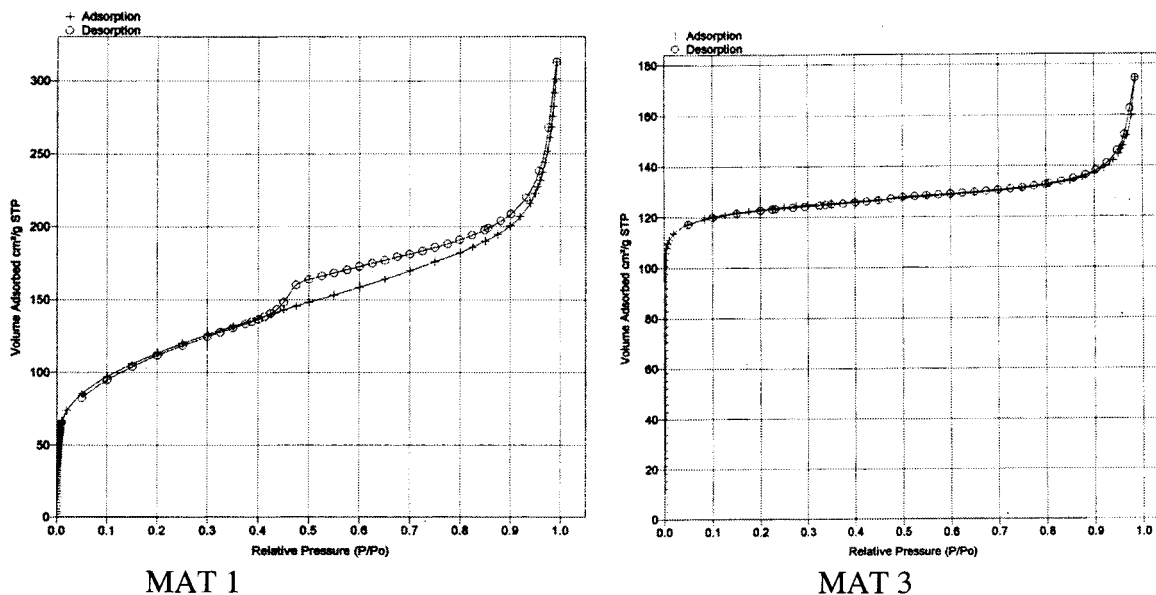


Figure 7. Nitrogen adsorption and desorption isotherms of MAT 1 and MAT 3.

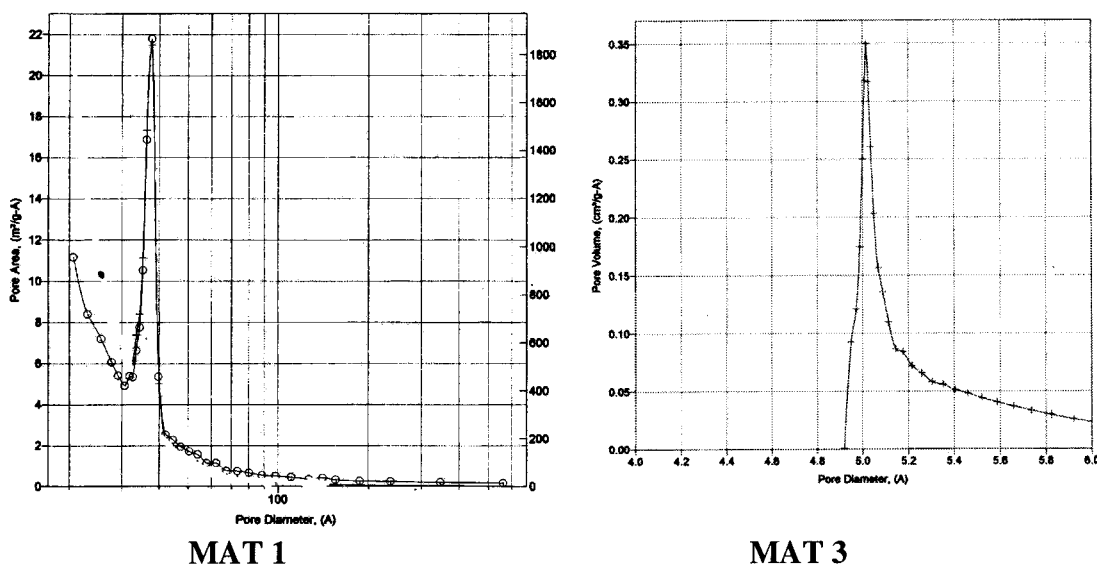


Figure 8. Mesopore-size distribution curve for MAT 1 and micropore-size distribution curve for MAT 3.

bipyridine, or counterion). The spontaneous color change after metal contact and the absorption spectrum featuring a MLCT transition are in agreement with the formation of iron(II) and copper(I) complexes. These features prove that the bipyridine units have kept their coordination ability after immobilization into the layered phosphonate frameworks.

Discussion

The present work reports the first example of zirconium phosphonates covalently pillared with bipyridine diphosphonic acid. To this goal, we have studied two approaches for the immobilization of 5,5'-bis(dihydroxyphosphoryl)-2,2'-bipyridine within the zirconium phosphonate frameworks. The first one consists of the coprecipitation of 5,5'-bis(dihydroxyphosphoryl)-2,2'-bipyridine and phosphorous acid with zirconium oxychloride in the presence of HF. It led to a pillared layered material formulated as $Zr(HPO_3)_{0.8}(O_3P\text{-bipy-}PO_3)_{0.6} \cdot 5.3H_2O$ with an interlayer spacing of 13.4 Å. Spectroscopic investigations (one- and two-dimensional experi-

ments ^{31}P MAS NMR) revealed that the product is a pure single phase in which the bipyridine pillars and the phosphite groups are randomly distributed. This material exhibits a high surface area of 420 m^2/g . Its porosity is essentially in the mesopore region (330 m^2/g) with an average diameter size of 40 Å. However, the microporous surface (90 m^2/g) is rather modest because this copolymerization method does not allow one to control the pillar/phosphite ratio to a sufficiently low value. However, the amount of pillars within the interlayer region can be finely tuned using the second approach based on the intercalation-exchange process that can take place into γ -ZrP. A 50% replacement of the dihydrogen phosphate groups by 5,5'-bis(dihydroxyphosphoryl)-2,2'-bipyridine affords a porous material with a high microporous surface (350 m^2/g) and a pore diameter size centered at 5 Å.

Whatever the method used for the preparation of the materials, infrared spectroscopy showed that the bipyridine moiety in the solids is essentially unprotonated because the N-H stretching bands at 1577 and 1276

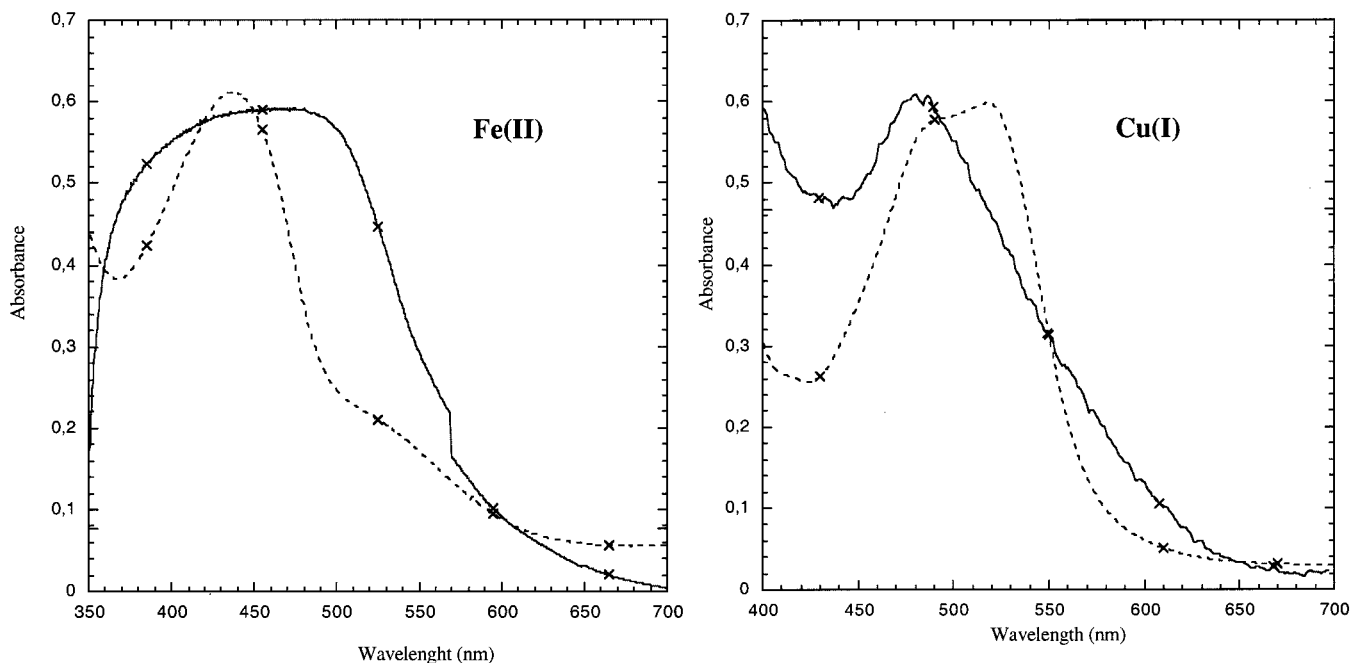


Figure 9. Overlay of the electronic absorption spectra of bipyridine (dotted line) and MAT 1 (solid line) after complexation with Cu(I) (left) and Fe(II) (right).

cm^{-1} are absent in the spectra. Furthermore, thermogravimetry indicates that the thermal stability of the ligand is high because its decomposition only occurs above 500 °C.

Preliminary experiments on the reaction of these bipyridine-containing materials with methanol solution of iron(II) and copper(I) have demonstrated that these metals can effectively bind to the immobilized bipyridine via coordination through its chelating nitrogen atoms.

Because of the large surface area in the microporous region along with the high coordination ability of the bipyridine, these materials offer promising perspectives in the field of supported ligands for catalysis or metal recovery. Studies are presently underway in our laboratory to investigate the catalytic performances of these bipyridine-containing materials. We also believe that the same approach might be conducted successfully with other valuable ligands with C_{2v} symmetry such as binaphthyl or oxazolidines derivatives.

In the future, one can envision that the inorganic framework can wrap a catalytic site, offering extra beneficial properties such as protection and selectivity in a manner similar to the well-organized protein matrixes in enzymes.

Experimental Section

Materials. Reagents used were obtained from Aldrich ($\text{ZrO}_2\text{Cl}_2 \cdot 8\text{H}_2\text{O}$, H_3PO_3) and Prolabo (concentrated hydrofluoric acid 40%) and used without further purification. 5,5'-Bis-(dihydroxyphosphoryl)-2,2'-bipyridine, $^{12}\text{Zr}(\text{HPO}_3)_2 \cdot 2\text{H}_2\text{O}$, $^{22}\text{Zr}(\text{PO}_4)(\text{H}_2\text{PO}_4) \cdot \text{H}_2\text{O}$,²³ and $\text{Cu}^{\text{I}}(\text{CH}_3\text{CN})_4\text{BF}_4$ ²⁴ were prepared as previously described.

Sample Characterization. Powder X-ray diffraction measurements were performed with a Siemens diffractometer

D5000 equipped with a monochromator using Cu $K\alpha$ ($\lambda = 1.5418 \text{ \AA}$). Fourier transform infrared spectra were recorded in pressed KBr pellets on a Bruker Vector 22 spectrometer. UV-vis absorption spectra were recorded on a Cary 5G Varian spectrophotometer.

Solid-state ^{31}P NMR spectra were recorded on a Bruker solid-state NMR DSX 400 spectrometer using double-bearing magic-angle spinning probe heads with 4-mm ZrO_2 rotors spinning at up to 15 Hz. Liquid ^{31}P NMR spectra were measured on an AC 200-MHz Bruker spectrometer.

The thermogravimetric analyses (TGA) were carried out under an air atmosphere at a heating rate of 2 °C/min with a Setaram TGA-DTA92. To measure the textural properties of the solids, they were first degassed at 200 °C under vacuum for 6 h. The surface measurements were made by nitrogen adsorption by means of a Micrometrics ASAP2010C apparatus.

Preparation of α -Zirconium Phosphite-(2,2'-bipyridine-5,5'-diphosphonate): (MAT 1) $\text{Zr}(\text{HPO}_3)_{0.8}(\text{O}_3\text{P-bipy-PO}_3)_{0.6} \cdot 5.3\text{H}_2\text{O}$. Two hundred milligrams (0.63 mmol) of 5,5'-bis-(dihydroxyphosphoryl)-2,2'-bipyridine and 2.54 g (31 mmol) of phosphorous acid were dissolved in 40 mL of DMSO in a Teflon beaker. The mixture was heated to 80 °C until total solubilization occurred. A solution of ZrF_6^{2-} was then prepared by dissolving 205 mg (0.64 mmol) of $\text{ZrOCl}_2 \cdot 8\text{H}_2\text{O}$ in 1.7 mL of concentrated HF (40%) in a separate plastic beaker (this represents a F/Zr ratio of 60) and was added to the phosphonic acids mixture, which resulted in a milky slurry. The mixture was kept at 80 °C for 16 h under a well-ventilated hood. During this time the volume was reduced to one-third of the original quantity and a white precipitate formed. The solid was filtered off and rinsed with DMSO, then with water, and finally with acetone. After the mixture dried in air for 1 day, 200 mg of a white compound was collected.

The pure zirconium (2,2'-bipyridine-5,5'-diphosphonate) (MAT 5) was prepared following the above procedure but in absence of phosphorous acid.

Topotactic Exchange Reaction with γ -ZrP (MAT 2 and MAT 3). A suspension of 100 mg (0.31 mmol) of γ -ZrP and 30 mg or 15 mg (95 μmol or 47.5 μmol) (cf. Table 2) of 5,5'-bis-(dihydroxyphosphoryl)-2,2'-bipyridine was refluxed in 20 mL of acetone/water (1/1) mixture for 4 days. The white precipitate was filtered off and washed several times with a hot mixture of acetone/water, 1/1 and then with acetone. The resulting solid was finally dried until constant weight at ambient temperature (100 mg).

(22) Alberti G.; Constantino, U.; Giulietti R. *J. Inorg. Nucl. Chem.* **1980**, *42*, 1062–1063.

(23) Poojary, D. M.; Sheizer, B.; Clearfield, A. *J. Chem. Soc., Dalton Trans* **1995**, 111–113.

(24) Kern, J. M.; Sauvage J.-P.; Weidmann, J.-L.; Armaroli, N.; Flamigni, P.; Balzani, V. *Inorg. Chem.* **1997**, *36*, 5329–5338.

To determine the composition of the solid, ^{31}P liquid nuclear magnetic resonance was used. About 10 mg of the solid was dissolved in a few drops of concentrated hydrofluoric acid (40%) and then diluted with deuterated DMSO (about 1 mL). The chemical shifts were referenced relative to 85% H_3PO_4 as an external reference. In the d^6 -DMSO/HF solution, the ^{31}P chemical shifts of 5,5'-bis(dihydroxyphosphoryl)-2,2'-bipyridine, phosphorous acid, and phosphoric acid were 7.6, 5.1, and 0 ppm, respectively.

Metal Ions Binding Experiments. Ten milligrams of the zirconium phosphonate sample was first compacted in a thin

pellet that was then dipped into a deoxygenated 10 mM solution of $\text{Fe}(\text{SO}_4)$ or $\text{Cu}^{\text{I}}(\text{CH}_3\text{CN})_4\text{BF}_4$ in methanol. The solid developed instantaneously a color change characteristic of the bipyridine metal complex. The UV-vis absorption spectrum of the solid was then recorded.

Acknowledgment. We thank Stephane Grolleau (IMN) for the porosity and surface area determinations and CNRS for financial support.

CM0005135